

Synthesis and optical properties of nickel-doped copper metaborate crystals

© A.D. Molchanova¹, E.M. Moshkina², M.S. Molokeev^{2,3,4}, E.V. Tropina¹, A.F. Bovina², K.N. Boldyrev¹

¹ Institute of Spectroscopy, Russian Academy of Sciences, 108840 Troitsk, Moscow, Russia,

² Kirensky Institute of Physics, Federal Research Center KSC SB, Russian Academy of Sciences, 660036 Krasnoyarsk, Russia

³ Siberian Federal University 660041 Krasnoyarsk, Russia

⁴ Scientific and Innovation Department, Kemerovo State University, 650000 Kemerovo, Russia

e-mail: nastyamolchanova@list.ru

Received August 16, 2021

Revised August 26, 2021

Accepted September 02, 2021

This work presents information on the growth and spectroscopic study of single crystals of copper metaborate doped with nickel $\text{Cu}_{1-x}\text{Ni}_x\text{B}_2\text{O}_4$ ($x = 0.05, 0.1$). In the absorption spectra of both crystals, satellites related to Cu centers distorted by impurity Ni atoms were observed near the lines of zero phonon transitions. Polarization studies in the isotropic ab -plane of the tetragonal crystal $\text{Cu}_{1-x}\text{Ni}_x\text{B}_2\text{O}_4$ show the presence of linear magnetic dichroism in the magnetically ordered state, which was previously observed both in manganese-doped and undoped copper metaborates CuB_2O_4 . The temperature of magnetic phase transitions into the collinear antiferromagnetic and into helicoidal structures, $T_N = 19.1$ K and $T^* = 8.6$ K, respectively, were determined from the temperature dependence of the dichroic signal.

Keywords: 3d-ions, crystal growth, optical spectroscopy, magnetic ordering, cuprates

DOI: 10.21883/EOS.2022.01.52994.41-21

Introduction

Copper metaborate CuB_2O_4 is of great interest due to its unusual physical properties. This compound crystallizes in the tetragonal space group $I4_2d$ (No.122), in which copper cations Cu^{2+} occupy two nonequivalent positions $4b$ and $8d$ [1] and form, respectively, two magnetic subsystems. Moreover, if several magnetic phase transitions occur in $4b$ subsystem in the temperature range $T < T_N = 21$ K, then $8d$ subsystem is quasi-one-dimensional and is not ordered even at helium temperatures. Studies of the magnetic structure of this compound have been performed for more than twenty years [2–7], but the rich temperature-field (B – T) phase diagram of the metaborate is still being studied and refined. In addition to the standard methods for studying the magnetic structure [2–7], which were applied to CuB_2O_4 , the spectroscopic method of linear dichroism (LD) was also used, which turned out to be informative and accurate. For example, using only this method, it was possible to register the splitting of the transition at $T^* = 9$ K into a helicoidal magnetic structure with two transitions at $T_1^* = 7.9$ K and $T_2^* = 8.5$ K [8]. Later, the same method was used to refine the magnetic structure in the vicinity of 2 K and to record three more low-temperature phase transitions [9]. Studies of CuB_2O_4 with partial replacement of Cu^{2+} cation by other magnetic 3d-ions are of great importance. It was not possible to observe the magnetoelectric effect in undoped copper metaborate, in $\text{Cu}_{0.97}\text{Ni}_{0.03}\text{B}_2\text{O}_4$ a significant increasing of magnetization and the appearance of electric polarization under the action of the magnetic field were observed [10].

The ability to control the magnetization of $\text{Cu}_{0.95}\text{Ni}_{0.05}\text{B}_2\text{O}_4$ using the electric field [11] was also demonstrated. Quite recently a theoretical analysis of the mechanism of the magnetoelectric coupling of the spins Ni^{2+} and Cu^{2+} with an external electric field in $(\text{CuNi})\text{B}_2\text{O}_4$ was carried out in the context of the influence of the crystal field and the spin-orbital interaction [12]. It is shown that the spins ordering in the plane ab of the crystal induces the electric polarization along c axis, which is predominantly due to nickel ions. However, the influence of Ni concentration on the electric polarization appearance was not studied, just as no studies were carried out on compounds $\text{Cu}_{1-x}\text{M}_x\text{B}_2\text{O}_4$ with another (except Ni) magnetic 3d-ion M . We have recently grown $\text{Cu}_{0.98}\text{Mn}_{0.02}\text{B}_2\text{O}_4$ crystal and studied its magnetic structure by the LD method [13]. It was shown that doping with manganese leads to the temperatures decreasing of magnetic phase transitions T_N and T^* , and no splitting of the phase transition at T^* is observed. This work relates to the growth and spectroscopic study of nickel-doped copper metaborate crystals $\text{Cu}_{1-x}\text{Ni}_x\text{B}_2\text{O}_4$ ($x = 0.05, 0.1$).

Crystal growth

Single-crystal samples $\text{CuB}_2\text{O}_4:\text{Ni}$ were obtained using the flux method in the spontaneous crystallization mode. The flux system looks like:

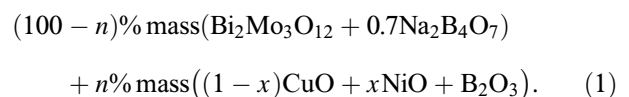


Table 1. Lattice parameters $\text{Cu}_{1-x}\text{Ni}_x\text{B}_2\text{O}_4$

	CuB_2O_4 [15]	$\text{Cu}_{0.95}\text{Ni}_{0.05}\text{B}_2\text{O}_4$	$\text{Cu}_{0.9}\text{Ni}_{0.1}\text{B}_2\text{O}_4$
a , Å	11.506	11.49707(11)	11.496293(95)
c , Å	5.644	5.624995(69)	5.624381(58)
V , Å ³	747.198	743.527(17)	743.345(14)

Fluxes were prepared by successive fusion of mixtures of oxide powders present in the flux system (1) in a platinum crucible at $T = 1000^\circ\text{C}$. At the homogenization stage, the fluxes were kept at $T = 1000^\circ\text{C}$ for 3 hours. Then, the temperature in the furnace was decreased, first rapidly (at a rate of $200^\circ\text{C}/\text{h}$) to $T = (T_{\text{sat}} - 10)^\circ\text{C}$ (here, $T_{\text{sat}1} = 840^\circ\text{C}$ and $T_{\text{sat}2} = 895^\circ\text{C}$ are saturation temperatures of the fluxes for $x_1 = 0.05$ and $x_2 = 0.1$, respectively, they were determined as described in [14]), then slowly (at rate of $3^\circ\text{C}/\text{day}$). After 3 days the crucible was removed from the furnace, flux was poured out. The grown single crystals were separated from the walls of the crucible and the remains of the flux with the help of 20% aqueous solution of nitric acid HNO_3 . Two samples were obtained with $x_1 = 0.05$ and $x_2 = 0.10$, the concentration of crystal-forming oxides was $n_1 = 35\%$ and $n_2 = 40\%$, respectively. The phase $\text{Cu}_{1-x}\text{Ni}_x\text{B}_2\text{O}_4$ was a high-temperature crystallizing phase in the wide temperature range (at least 40°C). The resulting $\text{Cu}_{1-x}\text{Ni}_x\text{B}_2\text{O}_4$ single crystals are elongated dark-blue prisms with sizes up to $3 \times 3 \times 10$ mm. There are cracks in the bulk of crystals caused by abrupt cooling after the growth stage.

The structure of the obtained $\text{Cu}_{1-x}\text{Ni}_x\text{B}_2\text{O}_4$ crystals was analyzed using X-ray powder analysis. As a result of the experiment the single-phase nature of the samples was confirmed and the parameters of the crystal lattice were obtained. The X-ray diffraction pattern was compared with that for undoped CuB_2O_4 from the powder database (map № 72-2024 PDF-2) [15]. The data are presented in the Table 1.

The lattice parameters decreasing in comparison with pure CuB_2O_4 probably indicates that nickel is present in the synthesized samples ($r(\text{Ni}^{2+}) = 0.69 \text{ \AA}$, $r(\text{Cu}^{2+}) = 0.73 \text{ \AA}$). However, when comparing the lattice parameters of samples with $x_1 = 0.05$ and $x_2 = 0.10$ the difference is observed only in the fourth decimal place. This probably means that the limit concentration of nickel has already been reached in the obtained samples.

Optical spectroscopy

The plane-parallel plates with orientation (001) were cut out for optical measurements, they were then polished. The samples thickness was $230 \mu\text{m}$. Absorption spectra in the optical range $11\,000\text{--}14\,000 \text{ cm}^{-1}$ were measured on Bruker IFS 125HR Fourier spectrometer with a resolution of 0.8 cm^{-1} . The samples were cooled in Cryomech ST403

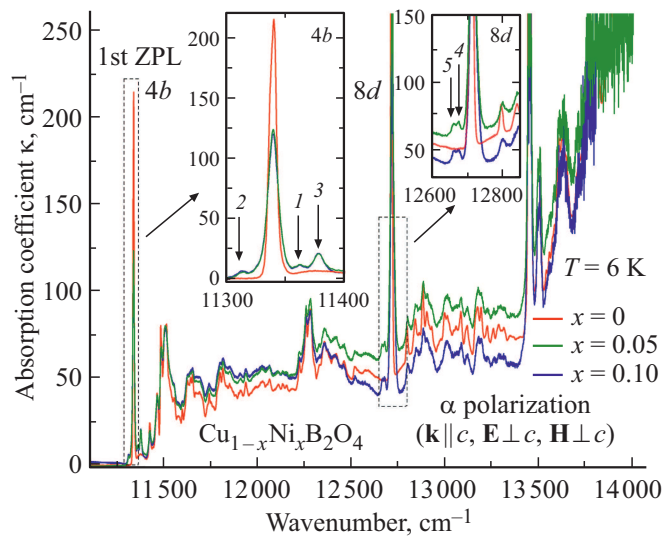


Figure 1. Absorption spectra of $\text{Cu}_{1-x}\text{Ni}_x\text{B}_2\text{O}_4$: $x = 0, 0.05, 0.1$ in α -polarization ($\mathbf{k} \parallel c$, $\mathbf{E} \perp c$, $\mathbf{H} \perp c$) at a temperature of 6 K. The arrows show the satellites of the first ZPL in $\text{Cu}_{1-x}\text{Ni}_x\text{B}_2\text{O}_4$ spectra associated with the distortion of the crystal lattice due to the inclusion of Ni^{2+} ion.

closed-cycle cryostat at temperatures $T < T_N$: 5–21 K. The absorption spectra of light propagating along the tetragonal axis c of the crystal were recorded. The LD signal was found as the difference of absorption coefficients κ (cm^{-1}) for light polarized along and perpendicular to the direction of antiferromagnetic spins $\{[110], [\bar{1}\bar{1}0]\}$ and $\{[110], [\bar{1}10]\}$, which below T_N are the source of optical anisotropy in the crystallographically isotropic plane (ab) of the tetragonal crystal (see details in paper [8]).

Results

Figure 1 compares the absorption spectra in α polarization ($\mathbf{k} \parallel c$, $\mathbf{E} \perp c$, $\mathbf{H} \perp c$) of pure and two doped $\text{Cu}_{1-x}\text{Ni}_x\text{B}_2\text{O}_4$ ($x = 0.05, 0.1$) copper metaborates. As in the spectrum of CuB_2O_4 , in the spectra of $\text{Cu}_{1-x}\text{Ni}_x\text{B}_2\text{O}_4$ one can observe zero-phonon lines (ZPL) of Cu^{2+} and their vibronic structure. In this case ZPL of Cu^{2+} in the spectra of doped metaborates are widened, and their maximum absorption coefficient is almost by two times lower than in undoped copper metaborate. In addition, near ZPL of Cu^{2+} in position $4b$ ($\nu = 11338 \text{ cm}^{-1}$) with lowest frequency, both on the left and on the right, one can see weak narrow satellites ($\delta\nu < 10 \text{ cm}^{-1}$) absent in the pure metaborate spectrum. The next ZPL $8d$ ($\nu = 12713 \text{ cm}^{-1}$) also has a satellite with more lower frequency and a double contour ($\nu_1 = 12676 \text{ cm}^{-1}$, $\nu_2 = 12661 \text{ cm}^{-1}$). Previously, a similar picture was observed for crystals of rare-earth aluminum borate doped with ytterbium [16–18], where the impurity atom distorted the ytterbium crystal environment, which led to ZPL shift. Here, probably, the satellites are caused by distortions of the Cu^{2+} positions due to the action of

Table 2. ZPL parameters of Cu(4*b*) 11339 cm⁻¹ and satellites in absorption spectra of Cu_{1-x}Ni_xB₂O₄ crystals: *x* = 0, 0.05, 0.1; Δ*v* is distance to main line, δ*v* is full width at half maximum (FWHM), *S* = ∫ κ(*v*)*dv* is integrated intensity (κ is absorption coefficient); *i* is number of the satellite from Fig. 1, while 0 is main ZPL

<i>i</i> (4 <i>b</i>)	0	1	2	3
<i>x</i> = 0.1				
Δ <i>v</i> , cm ⁻¹	0	22.66	-26.62	38.5
δ <i>v</i> , cm ⁻¹	10.43	4.93	6.13	9.44
<i>S</i> , cm ⁻²	1435.98	90.33	49.77	223.35
<i>S</i> _{<i>i</i>} / <i>S</i> _{total}		0.05	0.028	0.124
<i>x</i> = 0.05				
Δ <i>v</i> , cm ⁻¹	0	22.63	-25	38.56
δ <i>v</i> , cm ⁻¹	10.33	4.75	5.7	9.22
<i>S</i> , cm ⁻²	1446.03	89.124	45.03	219.326
<i>S</i> _{<i>i</i>} / <i>S</i> _{total}		0.05	0.025	0.122

Table 3. Parameters of ZPL satellites Cu(8*d*) 12714 cm⁻¹ Cu_{1-x}Ni_xB₂O₄: *x* = 0, 0.05, 0.1

<i>i</i> (8 <i>d</i>)	4	5
<i>x</i> = 0.1		
Δ <i>v</i> , cm ⁻¹	-41.1	-53.2
δ <i>v</i> , cm ⁻¹	11.4	10.1
<i>S</i> , cm ⁻²	121.1	107.1
<i>x</i> = 0.05		
Δ <i>v</i> , cm ⁻¹	-39.6	-52.5
δ <i>v</i> , cm ⁻¹	8.1	12.1
<i>S</i> , cm ⁻²	75.6	121.9

neighboring Ni²⁺ ions, which have ionic radius different from Cu²⁺ ions. The Tables 2, 3 list the parameters of all lines recorded in the vicinity of the first ZPL of subsystems Cu(4*b*) and Cu(8*d*), respectively. As expected, the integral intensity of satellite lines in Cu_{0.9}Ni_{0.1}B₂O₄ is higher than in Cu_{0.95}Ni_{0.05}B₂O₄, while the intensity of the main ZPL in Cu_{0.9}Ni_{0.1}B₂O₄ is lower. Thus, the total difference between the intensities of ZPL and satellites for two concentrations is equal to zero within the error.

The spectroscopic and structural data available are not enough to conclude that Ni²⁺ impurity ions occur in one or both crystallographic positions Cu²⁺, and (in second case) about a uniform distribution by positions. We performed analysis similar to that carried out in the paper [16].

Based on the assumption that Ni²⁺ can occupy both positions Cu²⁺, several nearest coordination spheres Cu²⁺ for centers 4*b* and 8*d* (Fig. 2, digits indicate the numbers of coordination spheres) were prepared. Also in the Table 4 the distances from the presumed Ni²⁺ center to the main positions Cu²⁺ are given. The smaller this distance is, the stronger the distortion of the crystal field is for a given Cu²⁺ ion, and the greater the spectral shift of the satellite is from the main line [16–18], while the intensity should be proportional to the number of equivalent Cu²⁺ centers around Ni²⁺.

From the data obtained, we can conclude that most of the satellites of the first ZPL Cu(4*b*) are associated with Ni in the position 8*d* (Ni(4*b*) in the first approximation have only one coordination sphere Cu(4*b*)). If we assume that Ni also enters 4*b* positions, then by the principle of reciprocity for Cu(8*d*) the closest crystallographic positions refer to Ni(4*b*). In this regard, we can assume the following distribution of nickel ions, which affect the environment of copper ions:

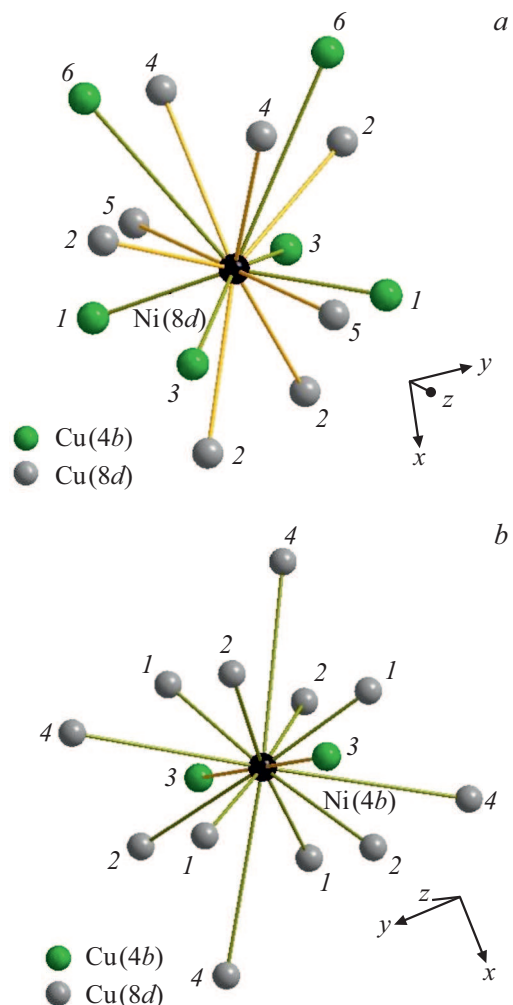


Figure 2. Cu²⁺ in coordination spheres Ni²⁺ in positions 4*b* (a) and 8*d* (b). Non-equivalent positions of copper are shown in different colors. The numbers designate the sequence numbers of the coordination spheres.

the farthest satellite Cu(4b) № 3 (see insert in Fig. 1) corresponds to the distortion by Ni(8d) atom, which is at a distance of 3.693 Å (Fig. 2, a, atom 1), satellite № 2 — to Ni(8d) atom at a distance of 4.647 Å (Fig. 2, a, atom 3), satellite № 1 — to Ni(8d) atom at a distance of 5.653 Å (Fig. 2, a, atom 6), or to Ni(4b) atom at a distance of 5.644 Å (Fig. 2, b, atom 3). The same comparison was made for the satellites of the first ZPL Cu(8d). The Table 4 gives data on the radii of the coordination spheres and associated satellites.

It is also important to note that the full spectrum of zero-phonon and vibronic transitions in undoped copper metaborate was recorded on a crystal 59 μm thick, since the lines were oversaturated on samples with greater thickness. In the present paper, the spectra of Cu_{1-x}Ni_xB₂O₄ were recorded on samples 230 μm thick; a lower thickness could not be achieved due to the brittleness of the sample. Thus, out of six ZPLs Cu²⁺, we managed to register three, and we do not have information about the parameters and satellites of the rest of ZPLs. Undoubtedly, the analysis of the complete spectral pattern could explain the question of the distribution of Ni²⁺ impurity centers over copper positions. The available data are not yet sufficient for this.

Figure 3 shows the LD spectra in the region of the first ZPL Cu(4b) with a frequency of about 11 340 cm⁻¹ in the absorption spectrum of Cu_{0.9}Ni_{0.1}B₂O₄. The color intensity map (Fig. 3, c) shows the appearance of linear dichroism below the temperature of $T = 19.1$ K, which indicates a magnetic phase transition into an antiferromagnetic structure [8,9,13]. Thus, the Neel temperature was determined. As in the paper [8], we believe that the magnetic Davydov splitting is responsible for the LD appearance. Dichroism is also observed on the satellite lines, it is clearly seen in the LD spectrum at 12 K (Fig. 3, b). The temperature of transition to the antiferromagnetic phase decreased in comparison with the pure metaborate, which is natural, since the addition of one more magnetic ion disorders the copper magnetic subsystem. At a temperature of $T^* = 8.6$ K, linear dichroism disappears, which apparently indicates a magnetic phase transition to a helicoidal structure, as was found for undoped metaborate [8]. Unlike pure metaborate, as well as Cu_{0.98}Mn_{0.02}B₂O₄ [13], with the temperature decreasing the dichroism does not appear up to the very low measured temperatures. It can be assumed that, at least up to 5 K, the magnetic structure of Cu_{0.9}Ni_{0.1}B₂O₄ remains simple helicoidal and does not become elliptical. However, for better understanding of the magnetic structure of nickel-doped copper metaborate at low temperatures, additional studies (magnetization measurements, neutron scattering, etc.) are required.

Conclusion

Cu_{1-x}Ni_xB₂O₄: $x = 0, 0.05, 0.1$ single crystals were grown by the flux method and studied. The parameters of the crystal lattice are determined. In the absorption spectra

Table 4. Distances (Å) between the supposed impurity centers Ni²⁺ and the nearest neighboring Cu²⁺ ions, number and position of Cu²⁺ ions are given in brackets in a given coordination sphere

№ coordination sphere	1	2	3	4	5	6
Ni(4b)	3.693 (4,8d)	4.647 (4,8d)	5.644 (2,4b)	5.653 (4,8d)	—	—
№ lines in Fig. 1	5	4	1			
Ni(8d)	3.693 (2,4b)	4.405 (4,8d)	4.647 (2,4b)	4.796 (2,8d)	5.644 (2,8d)	5.653 (2,4b)
№ lines in Fig. 1	3	4	2	4	1	

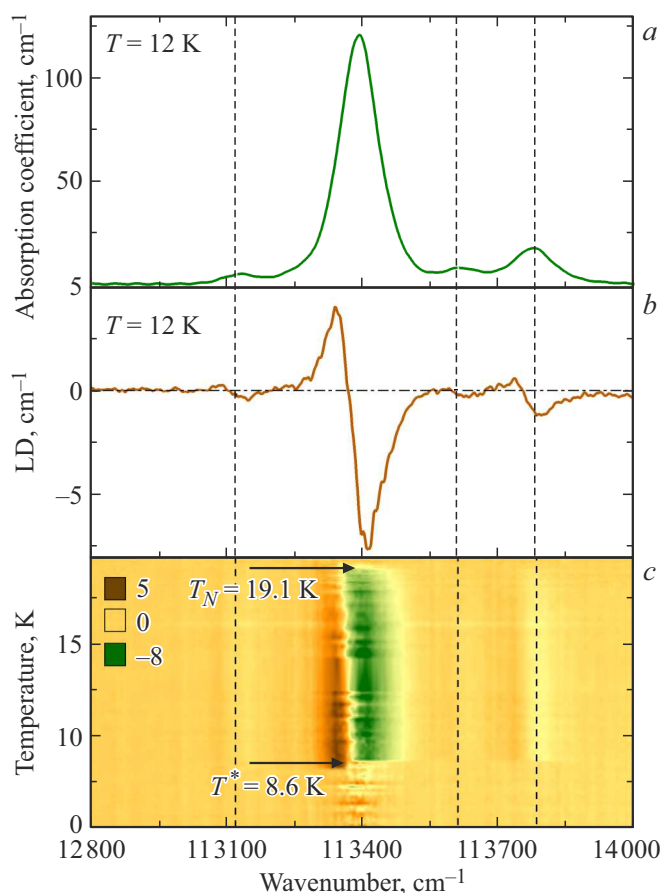


Figure 3. Spectra of Cu_{0.9}Ni_{0.1}B₂O₄ crystal in the region of the first exciton ZPL Cu(4b): absorption spectra at 12 K (a); LD spectra at 12 K (b); LD spectra presented as a color intensity map in the wavenumber — temperature axes (c).

of crystals near the ZPL of copper, satellites were observed, they belonged to Cu²⁺ centers distorted by nickel. The study of the satellites position, as well as the analysis of the possible positions of nickel in the nearest environment of copper, made it possible to assume the substitution of Ni²⁺ at the sites of the crystal lattice, which leads to a distortion of the crystal field and the appearance of a fine

structure near the ZPL of copper ions. As in undoped copper metaborate CuB_2O_4 , in the magnetically ordered state of $\text{Cu}_{0.9}\text{Ni}_{0.1}\text{B}_2\text{O}_4$ the linear dichroism associated with magnetic Davydov splitting was found. From the temperature dependences of the dichroism spectra the Neel temperature $T_N = 19.1\text{ K}$ and the temperature of transition to the magnetic helicoidal structure $T^* = 8.6\text{ K}$ are established. Unlike pure copper metaborate, no splitting of the transition at T^* and no transitions to the magnetic elliptical helicoidal structure were observed.

Funding

The study was performed with the support of Russian Science Foundation, RSF grant № 19-12-00413.

Conflict of interest

The authors declare that they have no conflict of interest.

References

- [1] M. Martinez-Ripoll, S. Martinez-Carrera, S. Garcia-Blanco // *Acta Crystallogr. Sect. B* 1971. V 27. P. 677. DOI: 10.1107/S0567740871002759
- [2] G. Petrakovskii, D. Velikanov, A. Vorotinov, A. Balaev, K. Sablina, A. Amato, B. Roessli, J. Schefer, U. Staub // *J. Magn. Magn. Mater.* 1999. V. 205. N 1. P. 105. DOI: 10.1016/S0304-8853(99)00449-7
- [3] M. Boehm, B. Roessli, J. Schefer, B. Ouladdiaf, A. Amato, C. Baines, U. Staub, G.A. Petrakovskii // *Physica B-Condensed Matter*. 2002. V. 318. N 4. P. 277. DOI: 10.1016/S0921-4526(02)00788-3
- [4] A.I. Pankrats, G.A. Petrakovskii, M.A. Popov, K.A. Sablina, L.A. Prozorova, S.S. Sosin, G. Shimchak, R. Shimchak, M. Baran // *Pis'ma v ZhETF*. 2003. T. 78. № 9. S. 569. (in Russian). DOI: 10.1134/1.1641486
- [5] B. Roessli, J. Schefer, G.A. Petrakovskii, B. Ouladdiaf, M. Boehm, U. Staub, A. Vorotinov, L. Bezmaternikh // *Phys. Rev. Lett.* 2001. V. 86. N 9. P. 1885. DOI: 10.1103/PhysRevLett.86.1885
- [6] M. Boehm, B. Roessli, J. Schefer, A.S. Wills, B. Ouladdiaf, E. Lelievre-Berna, U. Staub, G.A. Petrakovskii // *Phys. Rev. B*. 2003. V. 68. N 2. P. 024405. DOI: 10.1103/PhysRevB.68.024405
- [7] S. Martynov, G.A. Petrakovskii, B. Roessli // *J. Magn. Magn. Mater.* 2004. V. 269. N 1. P. 106. DOI: 10.1016/S0304-8853(03)00571-7
- [8] K.N. Boldyrev, R.V. Pisarev, L.N. Bezmaternykh, M.N. Popova // *Phys. Rev. Lett.* 2015. V. 114. N 24. P. 247210. DOI: 10.1103/PhysRevLett.114.247210
- [9] A.D. Molchanova, K.N. Boldyrev. Spektroskopiya vysokogo razresheniya nizkotemperaturnykh fazovykh perekhodov v metaborate medi // *Optika i spektroskopiya* 2019. T. 127. № 1. S. 33. (in Russian). DOI: 10.1134/S0030400X19070191
- [10] N.D. Khanh, N. Abe, K. Kubo, M. Akaki, M. Tokunaga, T. Sasaki, T. Arima // *Physical Review B*. 2013. V. 87. N 18. P. 184416. DOI: 10.1103/PhysRevB.87.184416
- [11] M. Saito, K. Ishikawa, S. Konno, K. Taniguchi, T. Arima // *Nature Materials*. 2009. V. 8. N 8. P. 634. DOI: 10.1038/nmat2492
- [12] M.V. Eremin, A.R. Nurmukhamedov // *JETP Letters*. 2021. V. 114. N 1. P. 35. DOI: 10.1134/S0021364021130063
- [13] A.D. Molchanova, K.N. Boldyrev, A.S. Erofeev, E.M. Moshkina, L.N. Bezmaternykh // *IOP Conf. Series: Journal of Physics: Conf. Series*. 2017. V. 917. P. 072003. DOI: :10.1088/1742-6596/917/7/072003
- [14] E. Moshkina, M. Molokeev, N. Belskaya, I. Nemtsev, A. Molchanova, K. Boldyrev // *CrystEngComm*. Accepted in 2021. DOI: 10.1039/D1CE00750E
- [15] G.K. Abdullaev, K.S. Mamedov // *Journal of Structural Chemistry*. 1981. V. 22. N 4. P. 637. DOI: 10.1007/BF00784113
- [16] M.N. Popova, K.N. Boldyrev, P.O. Petit, B. Viana, L.N. Bezmaternykh // *J. Phys.: Condens. Matter*. 2008. V. 20. P. 455210. DOI: 10.1088/0953-8984/20/45/455210
- [17] K.N. Boldyrev, M.N. Popova, L.N. Bezmaternykh, M. Bettinelli // *Kvantovaya elektronika*. 2001. T. 41. № 2. S. 120. (in Russian). DOI: 10.1070/QE2011v041n02ABEH014419
- [18] K.N. Boldyrev, M.N. Popova, M. Bettinelli, V.L. Temerov, I.A. Gudim, L.N. Bezmaternykh, P. Loiseau, G. Aka, N.I. Leonyuk // *Optical Materials*. 2012. T. 34. N 11. C. 1885. DOI: 10.1016/j.optmat.2012.05.021